Polymer Chemistry

ROYAL SOCIETY OF CHEMISTRY

PAPER

View Article Online
View Journal | View Issue

Open Access Article. Published on 20 8 2025. Downloaded on 2025/12/18 12:23:58.
This article is licensed under a Creative Commons Attribution-NonCommercial 3.0 Unported Licence.

Check for updates

Cite this: *Polym. Chem.*, 2025, **16**, 4120

Iron-initiated radical polymerization of acrylate monomers

Benedetta Palucci, * Adriano Vignali, Fabio Bertini and Simona Losio

Received 29th June 2025,
Accepted 18th August 2025

DOI: 10.1039/d5py00645g

rsc.li/polymers

In this study, we present a novel Fe–H initiated radical polymerization method for various acrylate monomers, using commercially available iron(III) acetylacetonate as a catalyst and tetramethyldisiloxane (TMDSi) as a reducing agent, under mild conditions. Methyl acrylate (MA) polymerization at 40 °C resulted in monomer conversion up to 65%, and significant molecular weights up to 400 kg mol^{-1} and unimodal dispersity. Rheological and mechanical studies revealed that the polymer exhibits strong viscoelastic properties and high elasticity, influenced primarily by the molecular weight. The polymerization of *N*,*N*-dimethylacrylamide (DMA), benzyl acrylate (BnA), *n*-butyl acrylate (*n*-BA), and *t*-butyl acrylate (*t*-BA) demonstrated similar control, with molecular weights ranging from around 200 to 700 kg mol^{-1} and conversions between 20% and 50%. The findings highlight the potential of Fe–H initiated polymerization as a sustainable and efficient alternative to conventional radical polymerization methods, offering advantages in scalability and control.

1. Introduction

Radical polymerization is a widely favoured process for producing high-molecular-weight polymers due to its versatility and compatibility with a broad range of monomers, including (meth)acrylates, (meth)acrylamides, acrylonitrile, styrenes, dienes, and various vinyl monomers.[1–5] It contributes significantly to global polymer production, accounting for nearly 45% of synthetic polymers and 40% of synthetic rubber produced annually.[3] Compared to metal-catalyzed insertion-coordination polymerization, radical polymerization tolerates unprotected functional groups in both monomers and solvents, enabling polymerizations in aqueous or protic media.[4] This adaptability, combined with straightforward operation, underscores its extensive utility in industrial applications.[6]

From a mechanistic standpoint, conventional radical polymerizations operate through a chain reaction process (Scheme 1a). The polymerization begins with the formation of radicals through an initiating event. The chain propagation then involves the sequential addition of monomer units to form propagating radicals, and the termination of the chain occurs when these propagating radicals self-react by combination or disproportionation.[7] In the realm of polymer chemistry, the quest for efficient and sustainable initiation methods for free radical polymerization processes remains an ongoing endeavour.[3] Traditional approaches often rely on peroxides or azo compounds as initiators, which raise concerns regarding safety, environmental impact, and efficiency.[8] For example, azo initiators like azobisisobutyronitrile (AIBN) decompose at around 65 °C, while peroxide initiators like benzoyl peroxide need temperatures above 80 °C for effective decomposition and polymerization initiation.[9] This high-temperature dependence impacts reaction kinetics and efficiency, demanding precise thermal control to prevent premature initiator decomposition and unwanted side reactions. Emerging alternatives aim to address these challenges by exploring novel initiation pathways.[10–13] One promising strategy is hydrometallation-based initiation, which utilizes metal-hydride complexes to generate reactive radicals under milder and non-toxic conditions. In 2014, the group of Baran has developed a novel

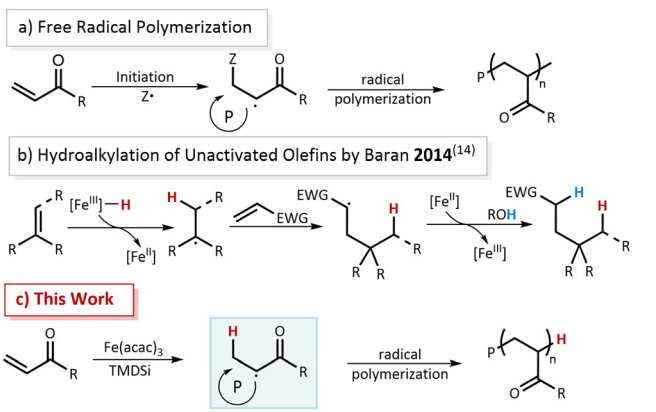

Scheme 1 Initiation methodologies for: (a) free radical polymerization, (b) hydroalkylation of olefins bearing electron-withdrawing groups (EWG), and (c) our proposed iron-initiated polymerization.

CNR-Istituto di Scienze e Tecnologie Chimiche "Giulio Natta" (SCITEC), via A. Corti 12, 20133 Milano, Italy. E-mail: benedetta.palucci@scitec.cnr.it

This journal is © The Royal Society of Chemistry 2025

Open Access Article. Published on 20 8 2025. Downloaded on 2025/12/18 12:23:58.
This article is licensed under a Creative Commons Attribution-NonCommercial 3.0 Unported Licence.

reductive olefin cross-coupling method, employing a metal-hydride hydrogen atom transfer (MHAT) mechanism (Scheme 1b).[14] The process begins with an iron catalyst that reacts with phenyl silane to produce an iron-hydride complex. This intermediate interacts with electron-rich olefins through a MHAT to produce a tertiary radical. These open-shell species are then captured by electron-poor olefins in a classic Giese-type reaction, seamlessly merging two olefins to create valuable sp^3-hybridized products. In contrast to the reported strategy, we envisioned generating radicals from electron-poor olefins to initiate the polymerization mechanism. However, the formation of a radical from electron-poor olefins *via* an *in situ*-generated iron hydride has not been previously reported, suggesting it may be unfeasible. Moreover, even if this step occurs, the radical intermediate is likely to undergo premature reduction by the silane, react with O_2, or form homodimers, thus preventing chain propagation. To overcome this challenge, we propose using a sub-stoichiometric amount of silane to trigger the formation of the initiation species without undergoing hydrogen atom abstraction. However, to the best of our knowledge, there are no reports on the polymerization of acrylates initiated by an iron-mediated hydrogen atom transfer.[15] Herein, we detail the development of a rapid, mild, and scalable radical polymerization methodology of methyl acrylate using an inexpensive, non-toxic, commercially available iron(III) acetylacetonate ($Fe(acac)_3$) catalyst with a silane initiator. Our goal is to underscore its importance as a sustainable and efficient polymerization strategy. The thermal, viscoelastic and mechanical properties of the obtained polymers have been investigated as well. Interestingly we pointed out the key role of molecular weight on these properties, in particular in terms of elasticity and tensile strength.

2. Experimental

Unless otherwise specified, all the manipulations were carried out on a double-manifold Schlenk vacuum line under a nitrogen atmosphere or in a nitrogen-filled MBraunUNIlab Plus glovebox. Unless otherwise stated, all other reagents were used without further purification.

2.1 Materials and methods

Methyl acrylate (MA; Sigma-Aldrich, 99%) was purified by drying over calcium hydride overnight, followed by distillation and degassing by three cycles of freeze–pump–thaw before being transferred to the glovebox. *n*-Butyl acrylate (*n*-BA; Sigma-Aldrich, 99%), *t*-butyl acrylate (*t*-BA; Sigma-Aldrich, 98%), benzyl acrylate (BnA; TCI, >97%), *N*,*N*-dimethylacrylamide (DMA; Sigma-Aldrich, 99%), *N*,*N*-dimethylformamide (DMF; Sigma-Aldrich, anhydrous over molecular sieves 99.8%) were purified by passing through a column of basic alumina and degassed by sparging with nitrogen before use. Toluene was dried by distillation from sodium under nitrogen atmosphere prior to use. 1,1,3,3-Tetramethyldisiloxane (TMDSi; TCI, >97%), iron(III) acetylacetonate (Sigma-Aldrich, ≥99.9%), Iron(II) acetylacetonate (Sigma-Aldrich, ≥99.9), phenylsilane ($PhSiH_3$; Sigma-Aldrich), 2,2,6,6-tetramethylpiperidine 1-oxyl (TEMPO, Sigma-Aldrich, 98%), *N*-fluoro-2,4,6-trimethylpyridinium tetrafluoroborate (NFTPB, Sigma-Aldrich, >95%) were used as received. Azobisisobutyronitrile (AIBN; Sigma-Aldrich, 98%) was recrystallized from methanol. The deuterated solvent for NMR measurements ($CDCl_3$) was used as received.

2.2 General procedures

2.2.1 General procedure for Fe–H initiated radical polymerization. In a glove-box, a one-dram reaction vial with a magnetic stir bar, $Fe(acac)_3$ (13.9 μmol, 4.9 mg, 0.5 equiv.) was mixed with acrylate (5.55 mmol, 200 equiv.). A stock solution of TMDSi was prepared in toluene (4.9 μL mL^{-1}). The vials were sealed and brough out of the box. The stock solution of TMDSi (1.23 μL, 6.937 μmol, 0.25 equiv.) in toluene (500 μL) was added to the reaction vial under nitrogen. The reaction vial was placed in a stirring hot plate at 40 °C to start the polymerization for the given time. A portion of the crude polymer was collected for the determination of conversion by ^{1}H NMR analysis, while the rest was precipitated in hexane.

2.2.2 General procedure for radical polymerizaton of MA initiated by AIBN. In a glovebox, $Fe(acac)_3$ (13.9 μmol, 4.9 mg, 0.5 equiv.) and AIBN (13.9 μmol, 2.3 mg, 0.5 equiv.) were added into a 2-dram vial followed by addition of MA (5.55 mmol, 200 equiv.) and toluene (500 μL). The vial was sealed and brought out of the box. The reaction vial was placed in an oil bath at 65 °C and the reaction was conducted for 2 hours. A portion of the crude polymer was collected for the determination of conversion by ^{1}H NMR analysis, while the rest was precipitated in hexane.

2.3 Characterization

2.3.1 Nuclear magnetic resonance (NMR) analysis. ^{1}H-NMR analyses were carried out using a 400 MHz Bruker Avance instrument at room temperature using *d*-chloroform ($CDCl_3$) as a solvent. For NMR analysis, about 10 mg of polymer was dissolved with deuterated solvent in a 5 mm NMR tube.

2.3.2 Size exclusion chromatography (SEC) analysis. SEC analyses were performed on a Waters Alliance system, using THF as the mobile phase, at 35 °C with a 0.6 mL min^{-1} flow. Sample concentration was set at 3 mg mL^{-1} and injection volume at 150 μL. Calibration of the curves was performed using polystyrene standards in the 162–800 000 g mol^{-1} range.

2.3.3 Differential scanning calorimetry (DSC). DSC analyses were carried out on a PerkinElmer (Waltham, MA, USA) DSC 8000 instrument. The samples were heated and cooled in the temperature range from −70 to 100 °C under nitrogen flow at scanning rate of 20 °C min^{-1}. T_g values were evaluated during the second heating scan (Fig. S6).

2.3.4 Thermogravimetric analysis (TGA). Thermogravimetric tests were performed by using a PerkinElmer (Waltham, MA, USA) TGA 7 instrument at heating rate of 20 °C min^{-1}. Each sample was investigated on the thermal range from 50 to 700 °C under nitrogen flow.

Open Access Article. Published on 20 8 2025. Downloaded on 2025/12/18 12:23:58.
This article is licensed under a Creative Commons Attribution-NonCommercial 3.0 Unported Licence.

Table 1 $Fe(acac)_3$ mediated conventional polymerization results of methyl acrylate at different polymerization conditions[a]

Entry	Cat.	MA/Fe/Si–H	Solvent (μL)	Conversion[b] (%)	M_n [c] (kg mol^{-1})	$Đ$ [c]
1[d]	$Fe(acac)_3$	200/1/0.5	500	60	290	1.9
2[e]	$Fe(acac)_3$	200/1/0.5	500	65	143	1.8
3	$Fe(acac)_3$	200/1/0.5	500	60	317	1.9
4	$Fe(acac)_3$	200/1/0.5	1000	27	216	1.8
5	$Fe(acac)_3$	200/1/0.5	1250	5	141	2.3
6	$Fe(acac)_3$	200/0.5/0.25	500	65	404	1.8
7	$Fe(acac)_3$	200/0.5/0.125	500	38	395	2.0
8	$Fe(acac)_3$ + TEMPO	200/0.5/0.25	500	—	—	—
9[f]	$Fe(acac)_2$	200/0.5/0.25	500	23	32	4.4
10[g]	$Fe(acac)_3$ + AIBN	200/0.5/—	500	95	110	2.7
11[g]	AIBN	200	500	98	120	2.7

[a] Reaction conditions: Si–H = 1,1,3,3-tetramethyldisiloxane (TMDSi), solvent = toluene; reaction time = 2 h; temperature = 40 °C; methyl acrylate (MA) = 5.55 mmol, 200 equiv. [b] Conversion from ^{1}H NMR analysis. [c] Determined by SEC in THF using PS standards. [d] Solvent = DMF. [e] Solvent = EtOH. [f] Oxidant = *N*-fluoro-2,4,6-trimethylpyridinium tetrafluoroborate (NFTPB). [g] Temperature = 65 °C; AIBN = 0.5 equiv.

2.3.5 Rheological analysis. The rheological behaviour of samples was analysed by dynamic measurements. A rotational rheometer TA Instruments (New Castle, DE, USA) AR 2000 operating in stress-controlled conditions, with circular plates (diameter = 25 mm), was used. Frequency sweep tests in the range between 0.01 and 625 rad s^{-1} were carried out at 110 °C applying a strain of 1%.

2.3.6 Dynamic mechanical thermal analysis (DMTA). Dynamic mechanical thermal analysis was carried out on an Anton Paar (Graz, Austria) MCR 702e instrument equipped with tension geometry. The samples for the DMTA were prepared by compression moulding in a hot-plate press at 110 °C applying a pressure of 50 bar for 5 min, afterwards the press plates were cooled by water to room temperature, obtaining films with a thickness of approximately 200 μm. Rectangular-shaped samples were tested setting a temperature ramp from −60 to 80 °C with a heating rate of 3 °C min^{-1}, a single frequency oscillation of 1 Hz and a strain amplitude of 0.1%.

2.3.7 Mechanical properties. The samples for the mechanical analysis were prepared as previously described in DMTA section. Tensile tests were carried out on dog-bone-shaped specimens with length overall of 75 mm, gauge length of 25 mm and width of narrow section of 4 mm at room temperature using a Zwick Roell (Ulm, Germany) ProLine Z010 dynamometer equipped with a load cell of 50 N at a constant deformation rate of 20 mm min^{-1}. Moreover, hysteresis experiments were performed at several strains by cyclically loading and unloading the specimens in uniaxial tension. The strain recovery (SR) was determined from the stress–strain curves as SR = $100(\varepsilon_a - \varepsilon_r)/\varepsilon_a$ where ε_a is the applied strain and ε_r is the strain in the cycle at zero load after the applied strain.

3. Results and discussion

Our investigation began by using a commercially available Fe $(acac)_3$ complex as a catalyst in combination with TMDSi as a reducing agent, to promote the formation of Fe–H species (Table 1). The polymerization of methyl acrylate in DMF achieved 60% monomer conversion, according to ^{1}H NMR spectrum, after 2 hours at 40 °C, with a molecular weight of 290 kg mol^{-1} (entry 1). We further explored the effect of the solvent among more and less coordinating ones (see Table S1 for a detailed list). Notably, the possibility of running the reaction in ethanol (entry 2) fully discards an anionic pathway and suggests a radical mechanism as depicted in Scheme 1c. In our conditions, the best compromise in terms of conversion, molecular weight and dispersity index seems to agree with the use of toluene (entry 3). In Fig. S1, the ^{1}H NMR spectrum of entry 3 is reported. Moreover, a study on the use of different toluene volumes shows that at lower amounts, the reaction kinetics slow down, resulting in conversion rates of 60%, 27%, and 5% in entries 3, 4, and 5, respectively. This effect is probably due to the reduced monomer concentration.

Interestingly, alongside the decrease in monomer conversion, there is also a noticeable reduction in the molecular weight of the polymer products (entries 4 and 5). When the reaction is performed at lower catalyst amount (entry 6) an increase of molecular weight up to 400 kg mol^{-1} is clear, keeping a monomodal dispersity (Fig. 1). Thus, we fixed 0.5 equiv. as proper amount of catalyst and decreased the amount

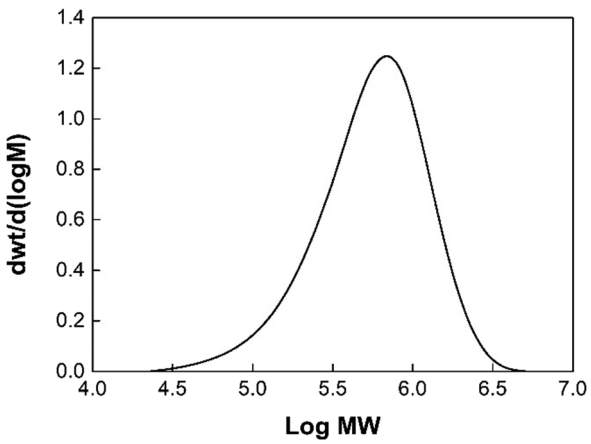

Fig. 1 SEC chromatogram of entry 6.

 This journal is © The Royal Society of Chemistry 2025

Open Access Article. Published on 20 8 2025. Downloaded on 2025/12/18 12:23:58.
This article is licensed under a Creative Commons Attribution-NonCommercial 3.0 Unported Licence.

of silane from 0.25 down to 0.125 equiv. No significant impact on the molecular weight can be observed despite a lower conversion (entry 7). On the basis of the previous experiments, it was determined that the optimal conditions were those in entry 6. As a result, the amounts of $Fe(acac)_3$ catalyst and TMDSi were adjusted to 0.5 and 0.25 equivalents, respectively, relative to MA. Under these conditions, the MA polymerization showed 65% monomer conversion in 2 hours at 40 °C with M_n = 404 kg mol^{-1} and $Đ$ = 1.8. A control experiment was conducted to confirm the intermediacy of radical species. When the reaction was performed in the presence of TEMPO as a radical scavenger, no conversion after 24 hours was observed (Table 1, entry 8). $Fe(acac)_2$ catalyst has been used as well in combination with the NFTPB as oxidant under the same polymerization conditions (entry 9). In this instance, iron(II) complex was oxidated to iron(III) and the addition of TMDSi generates the Fe–H initiator. Entry 9 leads to low conversion (23%), with molecular weight that is an order of magnitude smaller but higher dispersion $Đ$. As a preliminary investigation of the mechanism, we tested the reaction conditions in the absence of the iron complex or silane, or both, finding no monomer conversion, (Table S2). Moreover, for comparison, a reaction was conducted for 2 hours using AIBN as initiator, both in the presence and absence of $Fe(acac)_3$ (entries 10 and 11, respectively) at 65 °C, leading in both cases to almost complete conversion at the expense of lower molecular weight and broader dispersity compared to the Fe/Si system. These results suggest that $Fe(acac)_3$ acts as an initiator and does not influence the molecular weight or the polydispersity index, which are instead governed by the reaction temperature.

Once identified the best reaction conditions (Table 1, entry 6), a kinetic study has been conducted, and the results are summarized in Fig. 2.

A clear trend emerges, showing an increase in monomer conversion with longer reaction times. M_n does not increase proportionally with monomer conversion, remaining relatively consistent across entries 1 to 7, with values ranging from approximately 400 to 450 kg mol^{-1}. This points to that changes in reaction time do not significantly influence the molecular weight of the polymer product under the conditions tested, indicating a non-living polymerization. We extended the reaction time further, observing only a slight increase in conversion, while M_n decreased (Table S3, entry 8). This likely results from the continuous generation of reactive species during the reaction, leading to chain formation over time. As a results, after two hours, as monomer concentration decreases, newly formed chains become progressively shorter, causing a drop in M_n. The polydispersity index remains constant at about 1.8 for all entries, indicating a consistent molecular weight distribution regardless of reaction time. In summary, the data presented in Fig. 2 underscore the importance of reaction time in controlling monomer conversion while maintaining consistent molecular weight and dispersity, providing valuable insights for optimizing the polymerization process. Fe–H initiated radical polymerization was successfully employed with various monomers, as shown in Table 2, such as DMA, BnA, *n*-BA, *t*-BA. The monomer conversion after 2 h reaction time was evaluated by ^{1}H-NMR spectroscopy, all the spectra are included in the SI (Fig. S2–S5). Monomer conversions ranging from 20% to 50% were observed.

Interestingly, the use of *t*-butyl acrylate as a monomer resulted in the formation of high molecular weight polymer (M_n = 717 kg mol^{-1}).

The synthetized polymers present T_g values ranging from −45 and 50 °C (Fig. S6), and according to literature the T_g value depends on the chemical structures of the corresponding monomer.[16]

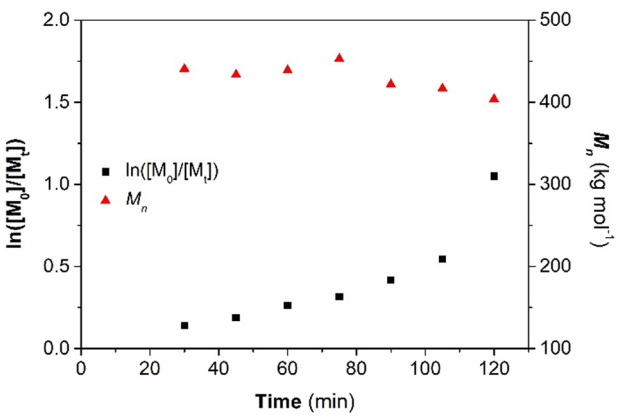

Fig. 2 $Fe(acac)_3$ mediated conventional polymerization of MA at different polymerization time performed at MA/Fe/Si–H = 200/0.5/0.25.

3.1 Thermal, viscoelastic and mechanical properties

The poly(methyl acrylate) entry 6, obtained using TMDSi in combination with $Fe(acac)_3$, exhibited the best molecular properties, in terms of high molecular weight and monomodal polydispersity, thus was selected to be extensively characterized by means of thermal, viscoelastic and mechanical analyses. The thermal properties of entry 6 were evaluated by differential scanning calorimetry and thermogravimetric analysis. DSC analysis highlighted that the sample is an amorphous polymer, characterized by a glass transition temperature (T_g) of 10 °C measured in the second heating scan (Fig. S7). TGA was performed to study the thermal stability of poly

Table 2 $Fe(acac)_3$ mediated conventional polymerization results of various monomers[a]

Entry	Monomer	Conversion[b] (%)	M_n[c] (kg mol^{-1})	$Đ$[c]	T_g[d] (°C)
12	DMA	24	430	1.8	−6
13	BnA	33	243	5.5	5
14	*n*-BA	50	292	3.0	−45
15	*t*-BA	20	717	1.7	50

[a] Reaction conditions: monomer/Fe/Si–H = 200/0.5/0.25; Si–H = 1,1,3,3-tetramethyldisiloxane (TMDSi); solvent = 500 µl toluene; reaction time = 2 h; reaction temperature = 40 °C. [b] Conversion from ^{1}H NMR analysis. [c] Determined by SEC in THF using PS standards. [d] Determined by DSC analysis.

Open Access Article. Published on 20 8 2025. Downloaded on 2025/12/18 12:23:58.
This article is licensed under a Creative Commons Attribution-NonCommercial 3.0 Unported Licence.

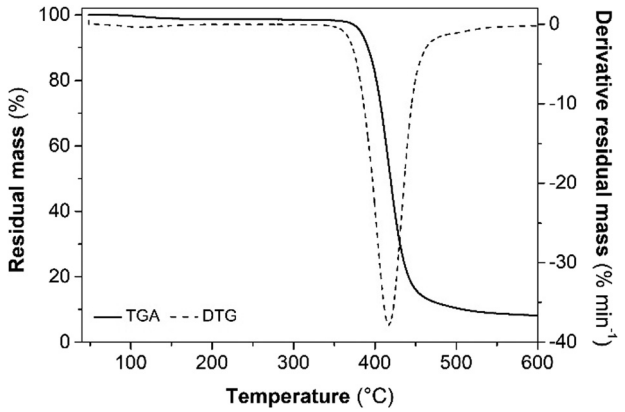

Fig. 3 TGA and DTG thermograms of entry 6.

(methyl acrylate). Fig. 3 shows the mass loss and the rate of mass loss from derivative thermogravimetry (DTG) as a function of the temperature. TGA and DTG curves allowed to determine some key parameters as the temperature at which the loss of 5% of mass is verified (T_d) and the temperature at which occurs the maximum rate of thermal degradation (T_p), (Table 3). In general, the poly(methyl acrylate) presents a good thermal stability with a single decomposition stage that occurs in the temperature range between 350 and 550 °C. The rheological analysis was performed to gain information on the relevant viscoelastic parameters such as shear storage modulus (G'), shear loss modulus (G'') and complex viscosity (η^*) of entry 6. Fig. 4 reports the moduli and η^* as a function of angular frequency (ω). It is evident that the high molecular weight dramatically affects the viscoelastic properties. In detail, this sample exhibits G' values very high and almost constant from 625 to 1 rad s^{-1} highlighting the predominance of elastic behaviour ($G' > G''$) due to abundant presence of entanglements. These physical crosslinks limit the chain mobility, as can be noticed evaluating the frequency in correspondence of crossover modulus (ω_{CO}), which is very low and equal to 0.025 rad s^{-1}. In fact, the inverse of ω_{CO}, which has the dimension of time, is substantially (at least in order of equal magnitude) to the longest relaxation time (disengagement time) of molecular chains and is proportional to the molecular weight, confirming the strong influence of this property on the molecular dynamics of the amorphous poly(methyl acrylate).

Table 3 Thermal properties, storage modulus in rubbery and glassy regions, molecular weight between adjacent entanglements and entanglement density of selected sample

Entry	T_g [a] (°C)	T_d [b] (°C)	T_p [b] (°C)	$E'_{-50\,°C}$ [c] (MPa)	$E'_{60\,°C}$ [c] (MPa)	M_e [c] (kg mol^{-1})	ν_e [c] (mol m^{-3})
6	10	382	417	3830	1.12	9	135

[a] Determined by DSC. [b] Determined by TGA. [c] Determined by DMTA.

Thus, the estimated high relaxation time of entry 6 is a clear indication of a strongly entangled polymer.[18] To better understand the viscoelastic properties with temperature and the role of entanglements as function of molecular weight, the selected sample was tested by dynamic mechanical thermal analysis. In Fig. 5 the poly(methyl acrylate) was investigated in terms of variation of extensional storage modulus (E') and loss factor ($\tan\delta$) as a function of temperature. Table 3 reports the extensional storage moduli of both samples measured in glassy region ($E'_{-50\,°C}$) and rubbery region ($E'_{60\,°C}$) at −50 and 60 °C, respectively. The rubbery region can be useful to quantify the entanglement density adapting the molecular theory of rubber elasticity proposed by Flory.[17] Therefore, the average molecular weight between adjacent entanglements (M_e) and the entanglement density (ν_e) of entry 6 was calculated from $E'_{60\,°C}$ in the rubbery plateau region using the following equations:

$$M_e = \frac{3\rho RT}{E'} \quad (1)$$

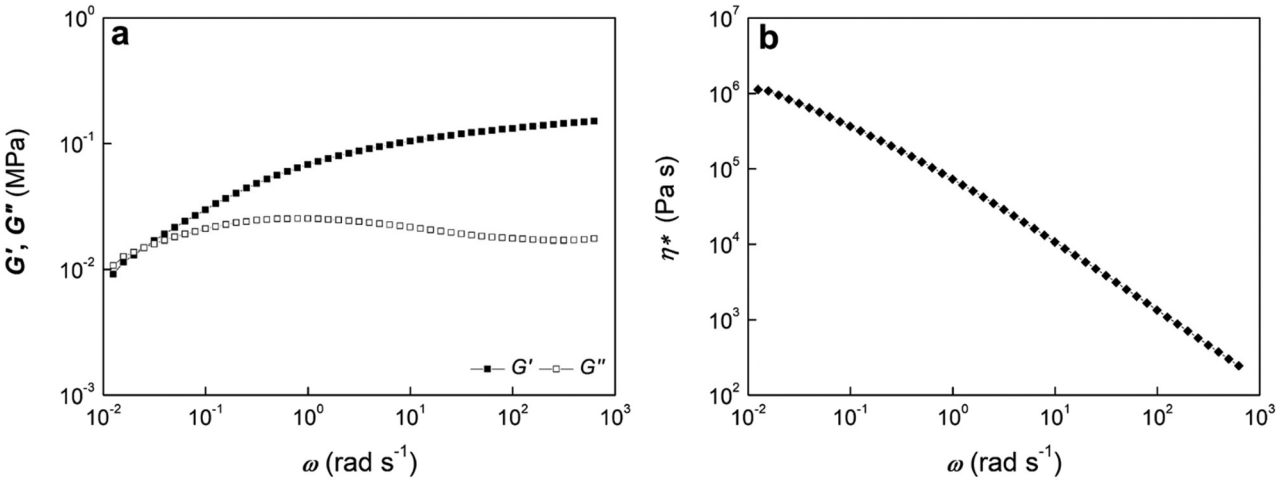

Fig. 4 (a) Shear storage and loss modulus and (b) complex viscosity as a function of angular frequency of entry 6.

This journal is © The Royal Society of Chemistry 2025

Open Access Article. Published on 20 8 2025. Downloaded on 2025/12/18 12:23:58.
This article is licensed under a Creative Commons Attribution-NonCommercial 3.0 Unported Licence.

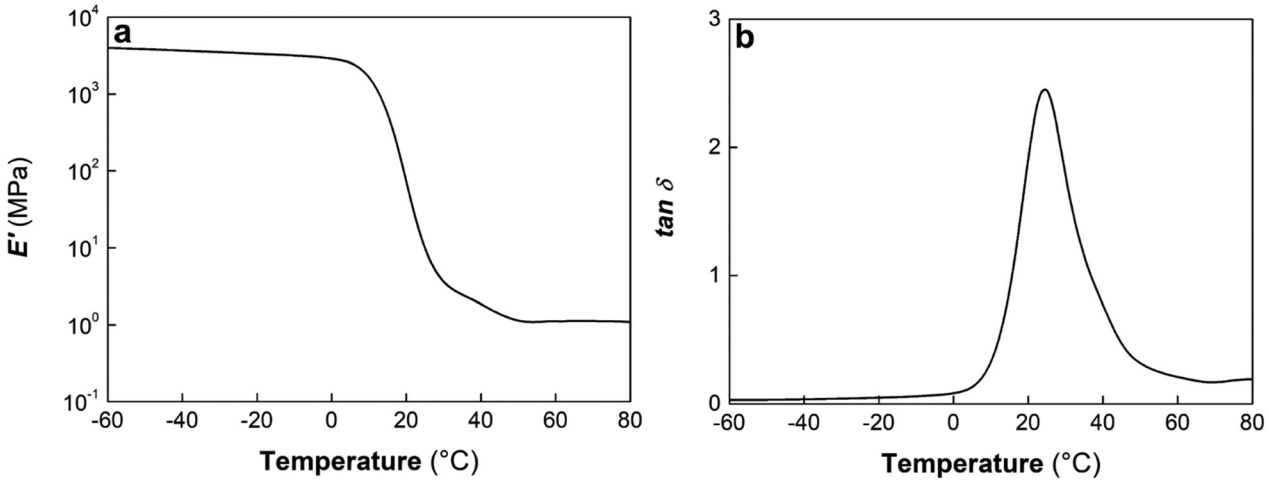

Fig. 5 (a) Extensional storage modulus and (b) loss factor as a function of temperature of entry 6.

$$\nu_e = \frac{\rho}{M_e} \quad (2)$$

where ρ is the density of polymethyl acrylates (1.22 g cm^{-3}),[18] R the universal gas constant (8.314 J K^{-1} mol^{-1}), T is the absolute temperature corresponding to E' in the rubbery plateau (333 K). The mechanical behaviour of sample was first analysed by uniaxial tensile test and the recorded stress–strain curves are shown in Fig. 6.

Tensile properties, such as Young's modulus (E), maximum strength (σ_{max}), elongation at break (ε) and fracture toughness (U_T), were averaged over five samples at least and reported in Table 4.

The mechanical performances of entry 6, synthetized using an Fe(acac)$_3$ complex as a catalyst in combination with TMDSi, are significantly affected by high molecular weight. In detail, this sample exhibits strain hardening behaviour, characterized by increasing stress as strain enhances, and considerable values of σ_{max} (2.32 MPa) and U_T (14.31 MJ m^{-3}) as consequence of high entanglements density that depends on high molecular weight and generates a physical elastic network.

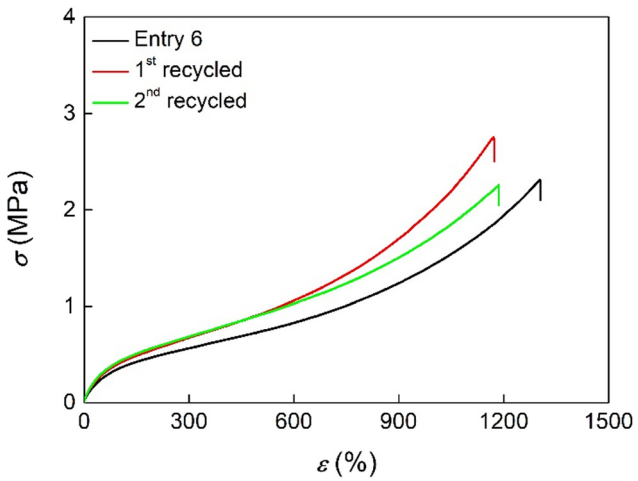

Fig. 6 Stress–strain curve in the uniaxial tensile test of the selected sample.

Table 4 Mechanical properties of selected samples

Entry	E (MPa)	σ_{max} (MPa)	ε (%)	U_T (MJ m^{-3})
6	1.7 ± 0.4	2.3 ± 0.1	1371 ± 94	14.3 ± 1.1
6-1st recycled	1.9 ± 0.2	2.8 ± 0.1	1213 ± 57	15.2 ± 1.7
6-2nd recycled	1.9 ± 0.4	2.1 ± 0.5	1168 ± 104	12.5 ± 1.5

Moreover, this sample shows E of 1.62 MPa and high ε equal to 1371%. This behaviour can be explained according to considerations reported by Diodati *et al.* on the effect of molecular weight on the mechanical properties of ultra-high molecular weight poly(methyl acrylate) showing that the mechanical properties are dramatically improved at high molecular weights.[19] The elastic property, that is the capacity of a material to recover its original shape and size after the removal of the applied force, was evaluated from hysteresis tests where the samples were cyclically loaded and unloaded to increasing strains. In Fig. 7 the stress–strain curves in the hysteresis experiments and the strain recovery, evaluated after the removal of the strain for each cycle, are shown.

Entry 6 exhibits an outstanding elastic recovery over the whole cyclic test. In particular, the strain recovery stands at about 90% from an applied strain of 160% up to 1200%. In details, the strain recovery is about 57% in the first cycles, and then gradually decreases up to 44% at 1200% strain, highlighting a high extent of irreversible deformation. The great elastic properties of entry 6 can be one more time attributed to the dense entanglements network caused by the high molecular weight.

The large number of entanglements generates a stronger elastic network that is more difficult to break even under high deformations and loads. A similar behaviour was observed for amorphous elastomeric ultra-high molecular weight polypropylenes with M_n higher than 1000 kg mol^{-1}, which exhibi-

Open Access Article. Published on 20 8 2025. Downloaded on 2025/12/18 12:23:58.
This article is licensed under a Creative Commons Attribution-NonCommercial 3.0 Unported Licence.

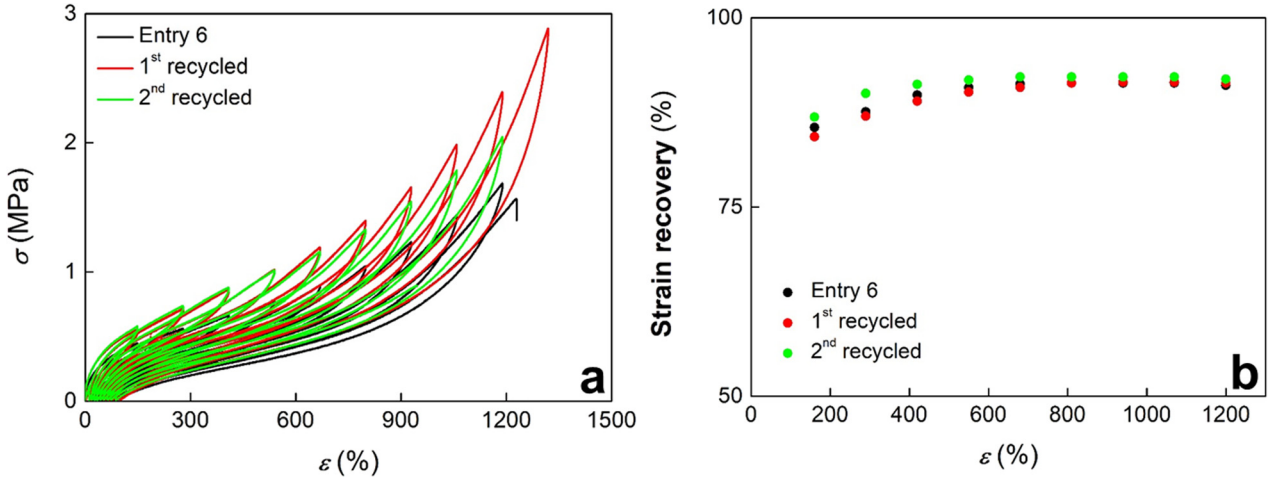

Fig. 7 (a) Stress–strain curves in the hysteresis test and (b) strain recovery as a function of different strains of pristine and recycled entry 6.

ted excellent elasticity (strain recovery ≈ 90%) after being cyclically stretched at 300% strain 10 times.[20] The reprocessability of entry 6, was evaluated by compression moulding the fractured specimens recovered at the end of tensile tests. The recycled samples with a 200 μm thickness were obtained at the same processing conditions of the initial preparation, thus in a hot-press at 110 °C and 50 bar for 5 min. The recycled samples were tested both in uniaxial tensile and hysteresis experiments in order to assess their recyclability. The mechanical properties and the stress–strain curves of the pristine and reprocessed entry 6 are shown for comparison purpose in Table 4 and Fig. 6, respectively. Both the pristine and recycled samples exhibit similar mechanical behaviour characterized by strain hardening region before breaking. Moreover, the tensile properties, in terms of E, σ_{max}, ε and U_T do not significantly change. As regards the step cyclic tensile tests (Fig. 7), the recycled samples preserve the remarkable elasticity and exhibit strain recovery nearly identical to the pristine polymer during all cycles at different strains.

Conclusions

In this work, we have successfully demonstrated a novel Fe–H initiated radical polymerization method for the synthesis of high-molecular-weight polyacrylates. By employing Fe(III) acetylacetonate in combination with TMDSi as a reducing agent, we achieved controlled polymerization under mild conditions, resulting in polymers with unimodal dispersity and high molecular weights. This approach was effective for a variety of monomers, including methyl acrylate, *N*,*N*-dimethylacrylamide, benzyl acrylate, *n*-butyl acrylate, and *t*-butyl acrylate, with monomer conversions ranging from 20% to 50%.

The Fe–H initiated polymerization of methyl acrylate produced high molecular weight polymers, exhibiting excellent thermal and mechanical properties. These improvements include greater thermal stability, increased tensile strength, remarkable elasticity and recyclability. Rheological and dynamic mechanical thermal analysis further confirmed the formation of robust polymer networks with strong viscoelastic behaviour, primarily influenced by the high molecular weight and entanglement density.

This methodology offers a sustainable and efficient alternative to traditional radical polymerization techniques, utilizing non-toxic, commercially available catalysts. The ability to control molecular weight and structure of the investigated polyacrylates makes this approach highly scalable and suitable for various industrial applications.

Author contributions

B. P.: conceptualization, investigation, validation, data curation, writing – original draft preparation, review, editing, funding acquisition. A. V.: data curation, validation, writing – original draft preparation, review, editing. F. B.: data curation, validation, writing – original draft preparation, review, editing. S. L.: supervision, writing – original draft preparation, review, editing. All authors have read and agreed to the published version of the manuscript.

Conflicts of interest

There are no conflicts to declare.

Data availability

The data supporting this article have been included as part of the SI: experimental section, ^{1}H NMR spectra, DSC thermograms. See DOI: **https://doi.org/10.1039/d5py00645g**. The raw data files are available in the FigShare repository at **https://doi.org/10.6084/m9.figshare.27223566**.

This journal is © The Royal Society of Chemistry 2025

Open Access Article. Published on 20 8 2025. Downloaded on 2025/12/18 12:23:58.
This article is licensed under a Creative Commons Attribution-NonCommercial 3.0 Unported Licence.

Acknowledgements

The authors thank Fulvia Greco and Daniele Piovani for their valuable cooperation in NMR and SEC analysis. B. P. thanks the Horizon Europe research and innovation program for the Postdoctoral Fellowship under the Marie Curie Grant Agreement (POLYFUN, No. 101062863).

References

1 C. Walling, *Free radicals in solution*, Wiley, New York, 1957.
2 C. H. Bamford, W. G. Barb, A. D. Jenkins and P. F. Onyon, *The kinetics of vinyl polymerization by radical mechanisms*, Academic Press, New York, 1958.
3 K. Matyaszewski and T. P. Davis, *Handbook of radical polymerization*, Wiley-Interscience, Hoboken, 2002.
4 G. Moad and D. H. Solomon, *The chemistry of radical polymerization*, Elsevier, Oxford, UK, 2nd edn, 2006.
5 B. Yamada, Free-Radical Addition Polymerization (Fundamental), in *Encyclopedia of Polymeric Nanomaterialsed*, ed. S. Kobayashi and K. Müllen, Springer, Berlin, Heidelberg, 2015.
6 P. Nesvadba, Radical Polymerization in Industry, in Encyclopedia of Radicals in Chemistry, *Biology and Materials*, 2012.
7 J. Brandrup, E. H. Immergut, E. A. Grulke (eds) *Polymer handbook*, 4th edn. Wiley, New York, 1999.
8 D. Braun, *Int. J. Polym. Sci.*, 2009, 1–10.
9 S. Guo, W. Wan, C. Chen and W. H. Chen, *J. Therm. Anal. Calorim.*, 2013, **113**, 1169.
10 F. Ehlers, J. Barth and P. Vana, in *Fundamentals of Controlled/Living Radical Polymerization*, ed. N. V. Tsarevsky and B. S. Sumerlin, The Royal Society of Chemistry, 2013, pp. 1–59.
11 1 T. P. Lodge, and P. C. Hiemenz, in *Polymer Chemistry*, 2nd ed., CRCPress: Boca Raton, 2007.
12 Z. Bartczak, *J. Polym. Sci., Part B: Polym. Phys.*, 2010, **48**, 276.
13 S. Mapari, S. Mestry and S. T. Mhaske, *Polym. Bull.*, 2021, **78**, 4075–4108.
14 J. Lo, J. Gui, Y. Yabe, C.-M. Pan and P. S. Baran, *Nature*, 2014, **516**, 343.
15 For an iron catalysed ATRP reaction please see: X. Pan, N. Malhotra, J. Zhang and K. Matyjaszewski, *Macromolecules*, 2015, **48**(19), 6948–6954.
16 F. Fleischhaker, A. P. Haehnel, A. M. Misske, M. Blanchot, S. Haremza and C. Barner-Kowollik, *Macromol. Chem. Phys.*, 2014, **215**, 1192.
17 P. J. Flory, *Polym. J.*, 1985, **17**, 1.
18 R. Casalini, D. Fragiadakis and C. M. Roland, *Macromolecules*, 2011, **44**, 6928.
19 L. E. Diodati, A. J. Wong, M. E. Lott, A. G. Carter and B. S. Sumerlin, *ACS Appl. Polym. Mater.*, 2023, **5**, 9714.
20 S. Losio, F. Bertini, A. Vignali, T. Fujioka, K. Nomura and I. Tritto, *Polymers*, 2024, **16**, 512.